INTERNATIONAL JOURNAL OF INTEGRATED ENGINEERING
ISSN: 2229-838X e-ISSN: 2600-7916

IJIE

Vol. 17 No. 6 (2025) 258-267
https://publisher.uthm.edu.my/ojs/index.php/ijie

Wavelength Optimisation in a Spectroscopy System for Wide-Range Uric Acid Detection

Afiqah Yaacob[1], Nor Hafizah Ngajikin[1]*, Nurfatihah Che Abd Rashid[1], Siti Hajar Aminah Ali[1], Maslina Yaacob[1], Nurfarina. Zainal[1], Ian Yulianti[2], Noran Azizan Cholan[1]

[1] *Faculty of Electrical and Electronic Engineering, Universiti Tun Hussein Onn Malaysia, 86400 Batu Pahat, Johor, MALAYSIA*

[2] *Department of Physics, Universitas Negeri Semarang, 50229 Semarang, INDONESIA*

*Corresponding Author: norhafizah@uthm.edu.my
DOI: https://doi.org/10.30880/ijie.2025.17.06.021

Article Info

Received: 30 May 2025
Accepted: 13 September 2025
Available online: 30 December 2025

Keywords

Uric acid detection, spectroscopy, visible spectrum, reagent-free

Abstract

This study demonstrates a wide linearity range for uric acid sensing in the visible and near-infrared spectrum using direct spectroscopy detection, eliminating the need for enzymes or reagents. The system was experimentally tested across a uric acid concentration range of 10 to 200 mg/dL, exhibiting excellent performance in linearity, sensitivity, and accuracy, with optimal results observed at a wavelength of 950 nm. At this wavelength, the sensor achieved a linearity of 0.9694, sensitivity of 0.0034 $(mg/dL)^{-1}$, and accuracy of 97.42%. Compared to the previous developments, this work validates the improved linearity range performance and offers rapid response times due to its reagent-free design. The proposed sensor shows strong potential for efficient real-time monitoring of uric acid over a wide concentration range.

1. Introduction

Uric acid is a byproduct of purine metabolism, which is 2,6,8-trihydroxypurine and appears in both keto and enol forms, as illustrated in Fig. 1 [1]. In healthy individuals, serum uric acid levels typically range from 2.18 to 7.7 mg/dL and 25 to 74 mg/dL in urine [2], [3]. Elevated levels, exceeding 7 mg/dL in men and 6 mg/dL in women [4], can indicate hyperuricemia, which is linked to conditions like gout, nephrolithiasis, diabetes mellitus, cardiovascular disease, hypertension, obesity, and chronic kidney disease [5], [6], [7], [8], [9], [10]. In food processing applications, uric acid is an indicator of contamination in food products like flour, cereals, and spices [11], [12], [13], [14], [15]. Thus, uric acid detection and measurement are needed in these applications. Several methods are used for uric acid detection such as electroanalytical [16], high-performance liquid chromatography (HPLC) [17], and spectroscopy [18], [19]. Electroanalytical techniques offer a simple detection system but rely on uricase, which normally faces enzyme mobilization and reproducibility challenges under controlled conditions [16]. While HPLC is a rapid detection method but limited by low sample throughput, and high cost, making it unsuitable for routine clinical analysis [20]. On the other hand, a spectroscopy technique offers a simple detection with a broad linearity range. It does not require the disposal of testing components, making it eco-friendly and more economical [18], [19].

In literature, uric acid detection for a wide linearity range has been explored independently in the ultraviolet (UV), visible, near-infrared (NIR) and short-wavelength-infrared (SWIR) spectra. In the UV spectrum, detection at a 300 nm wavelength has demonstrated a detection range between 9 to 90 mg/dL with linearity of 0.9633 and sensitivity of $0.0063(mg/dL)^{-1}$ [21]. Other work by N Norazmi et al, 2017 exhibited a wider linearity range of uric acid detected at 294.46 nm wavelength for a concentration between 40 to 100 mg/dL with a better sensitivity

performance of 0.01(mg/dL)$^{-1}$ [22]. The results analysed using Spectrasuite software also confirmed that uric acid could be detected at a constant UV wavelength with a fast response time of around 3 seconds [22]. Although these works demonstrate a good performance in uric acid detection, spectroscopy works in the UV spectrum requires a specialized UV-transparent cuvette made of quartz or UV-grade plastic which consumes higher cost [23]. While, in the SWIR spectrum, spectroscopy operated at 1550 nm wavelength measured uric acid in concentrations ranging from 3 to 15 mg/dL in artificial blood samples. The linear regression analysis between uric acid concentration and the digital output shows a linearity of 0.9710 and a normalised sensitivity of 0.0036 (mg/dL)$^{-1}$, providing a reliable and convenient option for uric acid detection without using any reagents [24]. Similar to the UV spectroscopy system, the system requires a SWIR-transparent sample compartment, which is normally more expensive compared to the visible and NIR transparent cuvette [25], [26].

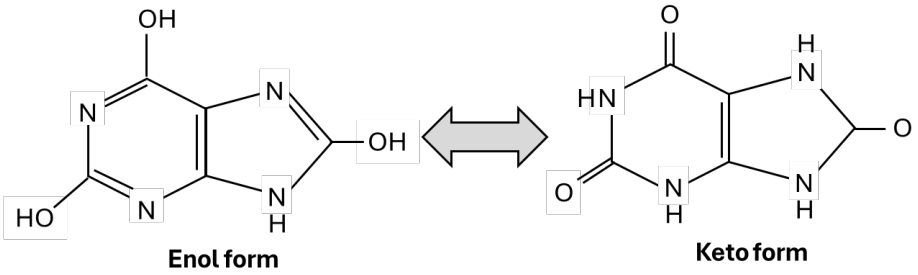

Fig. 1 *Uric acid chemical structure [1]*

The economic components of the visible and NIR spectroscopy system have attracted an exploration of uric acid detection in this region. Detection of 2 to 10 mg/dL uric acid in insect-infested food at 520 nm wavelength has demonstrated a colourimetric method for food quality by analyzing the potassium ferricyanide reaction with phenyl hydrazone to form an unstable chromophore. The technique achieved high linearity, R^2 of 0.9940 and sensitivity of 0.0103 (mg/dL)$^{-1}$ [27]. The same 520 nm wavelength was demonstrated for a colourimetric sensor for uric acid and H_2O_2 detection using mercaptosuccinic acid-modified copper nanoparticles (CuNPs). Uric acid or H_2O_2 causes mercaptosuccinic acid to cleave from CuNPs, triggering particle aggregation and transforming into violet. With a handheld photometer, uric acid was measured across a 0.08 to 75.65 mg/dL range, highlighting its potential for on-site diagnostics [2]. In other work, a study on the unreacted Ce4+ with methyl orange at 505 nm has demonstrated a sensitivity of 4.2703 (mg/dL)$^{-1}$ with a linearity of 0.8659, suitable for applications requiring moderate precision and accuracy [28]. In the same visible spectrum region, 15 to 85 mg/dL uric acid concentration in human urine has been experimentally demonstrated using a visible spectroscopy system at 460 nm wavelength using NaOH as its reagent, achieving 96.62% accuracy at 90 seconds response time [29]. Although these developed systems are effective, they rely on the reaction of reagents and enzymes that require a complex sample preparation process and time [27]. Thus, reagentless spectroscopy offers a simple preparation process and eliminates the need for chemical reaction time.

Uric acid detection using a reagentless spectroscopy system that works in the visible and NIR spectrum has been analyzed for a low concentration range between 2 to 10 mg/dL with a linearity of 0.9820 and sensitivity of 0.0380 (mg/dL)$^{-1}$, attributed to the relatively low molar attenuation coefficient in this spectral range [30]. In this work, the wavelength optimization of the spectroscopy system for uric acid detection in the visible and NIR spectrum has been conducted for a high concentration range between 10 to 200 mg/dL. As aforementioned, molar absorptivity or attenuation coefficient, ε dictates how efficiently a substance absorbs light at a specific wavelength [31]. This study improves the system's linearity range by optimizing the light source wavelength, making it suitable for applications involving broad concentration ranges in biological samples.

2. Experiment

2.1 Experimental setup

A schematic diagram of the experimental setup used to measure uric acid concentration is illustrated in Fig. 2. The configuration includes a light source (Ocean Optics deuterium halogen (DH)-mini light source), cuvette holder, spectrometer (Ocean Optics HR4000CGUV-VIS spectrometer), and a computer equipped with OceanView software. For this experiment, the cuvette holder is designed to accommodate a plastic cuvette with a 10 mm optical path, facilitating a linear trajectory for the light to pass through from the light source to the spectrometer. The spectrometer subsequently captures the output spectrum from the cuvette, and data analysis is performed

Int. Journal of Integrated Engineering Vol. 17 No. 6 (2025) p. 258-267

using OceanView software. The experimental apparatus was securely mounted on a vibration-free optical table to minimise measurement error.

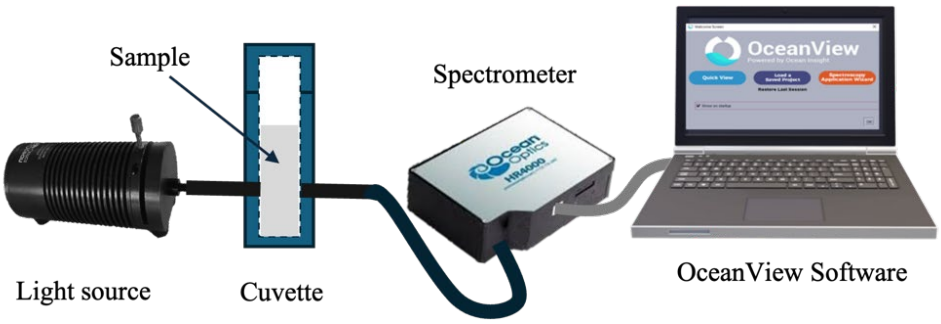

Fig. 2 *Experimental setup*

2.2 Sample Preparation

A 200 mg/dL uric acid stock solution was prepared and used to make a range of diluted solutions (10–200 mg/dL). In this work, uric acid powder (≥99%, Sigma-Aldrich) was accurately weighed at 2.000 g, as shown in Fig. 3(a). The powder was dissolved in 1 L of deionized water at a controlled room temperature of 25 °C. As depicted in Fig. 3(b), initial sedimentation of the powder at the bottom of the beaker was observed, indicating incomplete dissolution. To ensure complete dissolution, a magnetic stirrer (Stuart UC152) was used, with the stir setting adjusted to level 4, corresponding to approximately 500–600 rpm, for 3 minutes in a 1,000 mL beaker. A standard 25 mm PTFE-coated stir bar was employed during the stirring process. After 3 minutes of stirring, as depicted in Fig. 3(c), no visible powder remained, confirming the homogeneity of the solution. Subsequently, working standards of uric acid, ranging from 10 to 200 mg/dL, were prepared from the stock solution using 50 mL containers. The necessary dilutions were calculated following equation (1) to obtain the desired concentrations [32].

$$C_1V_1 = C_2V_2 \tag{1}$$

Where C_1 is the pre-dilution solution concentration in mg/dL, V_1 is the pre-dilution solution volume (mL), C_2 is the post-dilution solution concentration in mg/dL, and V_2 is the post-dilution solution volume (mL). These samples were then transferred into a cuvette for measurement as shown in the experimental setup in Fig. 2. Table 1 presents the required volumes of stock solution and deionized (DI) water needed to prepare the samples.

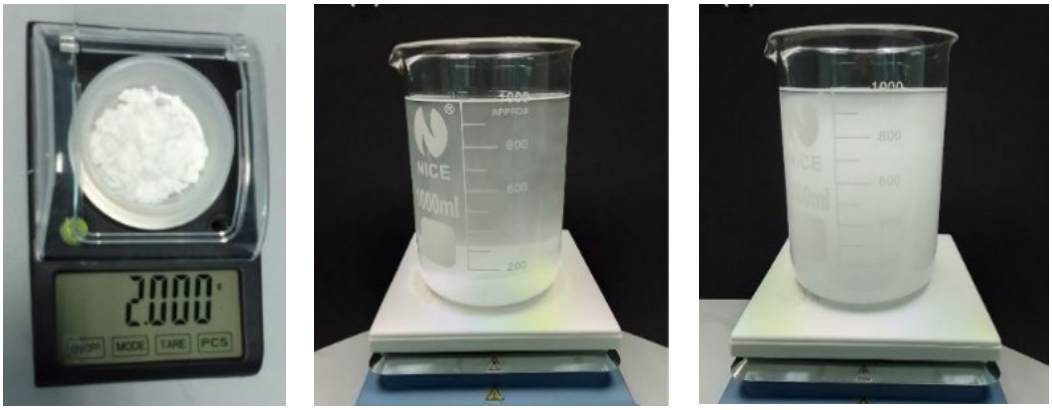

(a) **(b)** **(c)**

Fig. 3 *Preparation of 200mg/dL uric acid stock solution by (a) weighing uric acid powder on a scale uric acid stock solution; (b) before stir; and (c) after sti*

Table 1 *Uric acid diluted concentration and its corresponding DI water addition*

Pre-dilution concentration (mg/dL)	Pre-dilution Volume (mL)	Addition of DI water Volume (mL)	Post-dilution concentration (mg/dL)
200	2.5	47.5	10
200	5.0	45.0	20
200	7.5	42.5	30
200	10.0	40.0	40
200	12.5	37.5	50
200	15.0	35.0	60
200	17.5	32.5	70
200	20.0	30.0	80
200	22.5	27.5	90
200	25.0	25.0	100
200	27.5	22.5	110
200	30.0	20.0	120
200	32.5	17.5	130
200	35.0	15.0	140
200	37.5	12.5	150
200	40.0	10.0	160
200	42.5	7.5	170
200	45.0	5.0	180
200	47.5	2.5	190
200	50.0	0.0	200

3. Results and Discussion

The absorbance of light by uric acid adheres to the Beer-Lambert law, which correlates light attenuation with the sample's properties, specifically transmittance, T and absorbance, A. T represents the ratio of light intensity passing through the sample cuvette (with sample) to the reference cuvette (without sample). A and T are related where A is the logarithm of the inverse of T, meaning a lower T value corresponds to a higher A value and vice versa. These two variables are related to the uric acid sample concentration, c, path length, b and the molar attenuation coefficient, ε as in equation (2) [30], [33]. In this work, the system will be optimized for its operating wavelength since the ε is wavelength-dependent, thus the system will respond uniquely at the different operating wavelengths.

$$A = log\frac{1}{T} = \varepsilon bc \tag{2}$$

Fig. 4 presents the output intensity spectrum of the sensor across a wavelength range of 400 to 1000 nm. The output intensity is observed as varying uric acid concentrations from 10 to 200 mg/dL, corresponding to specific absorption lines that indicate the presence of uric acid in the sample. The graph reveals that intensity decreases linearly as the uric acid concentration increases, implying that greater concentrations lead to higher losses, thereby reducing the system's output light intensity [34]. This result agrees with the Beer Lambert's law [22]. Further analysis of the system absorbance spectra in Fig. 5 shows that absorbance increases linearly with uric acid concentration, with minimal absorption variation within the 450 to 650 nm range. In general, the absorbance value for all concentrations falls within an ideal range which is higher than 0.1. Beyond 650 nm wavelength, particularly in the NIR region, absorbance begins to gradually increase.

Int. Journal of Integrated Engineering Vol. 17 No. 6 (2025) p. 258-267

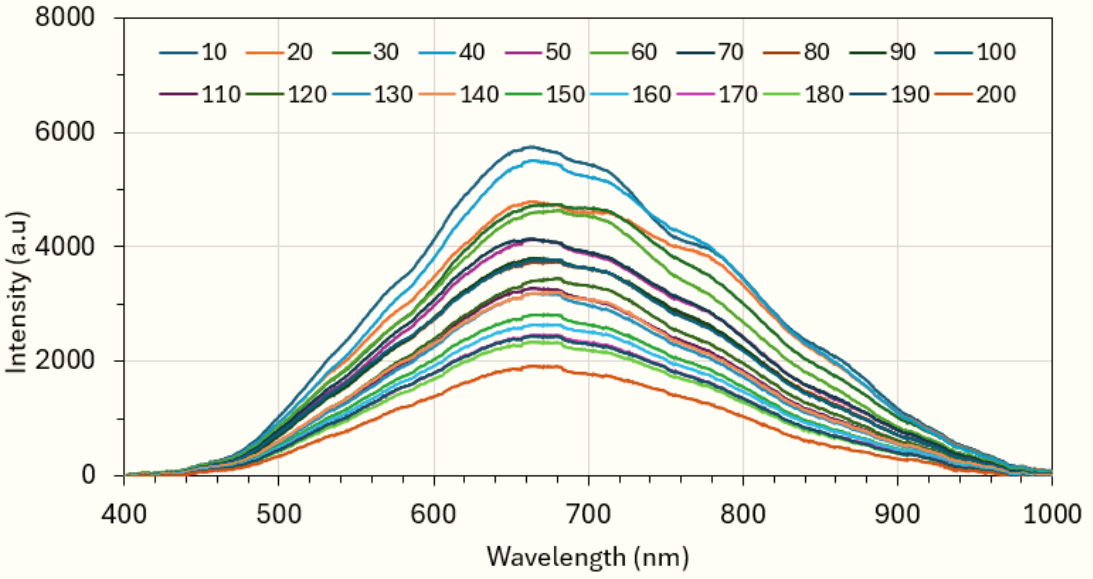

Fig. 4 *Output intensity spectrum as a function of wavelength for different uric acid concentrations*

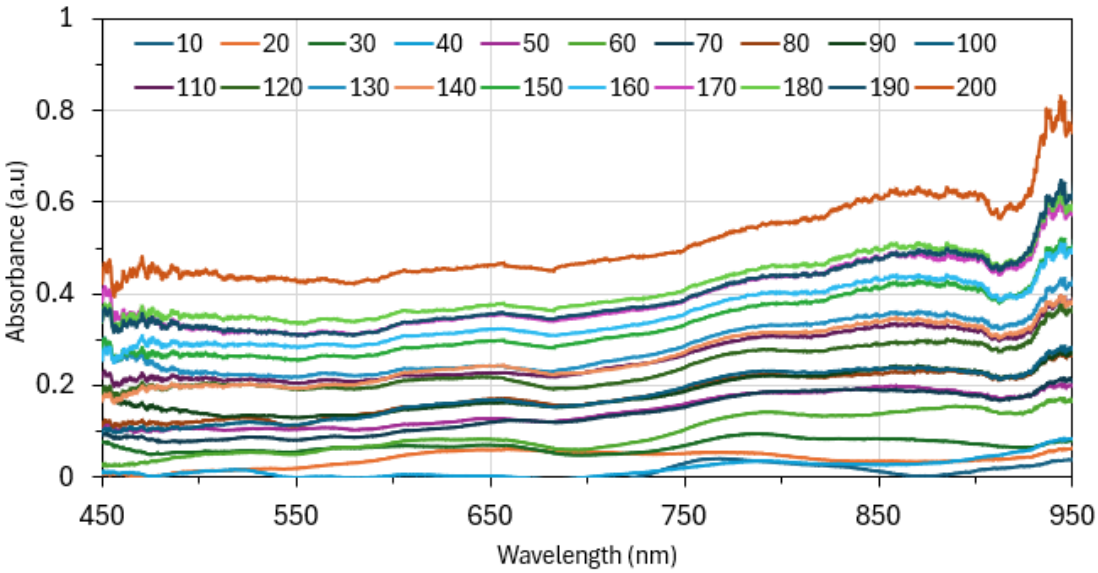

Fig. 5 *Absorbance as a function of wavelength for different uric acid concentrations*

Next, the system linearity, sensitivity, and accuracy performances are analyzed from the absorbance spectra for every 5nm sample wavelength for uric acid concentration from 10 mg/dL to 200 mg/dL. The system linearity, R^2 is obtained from the linear regression analysis of the absorbance curve for a different value of uric acid concentration [34]. While the system sensitivity is calculated from the slope of the graph [34]. While for the accuracy analysis, the calculation is carried out using equation (3) [29], [33].

$$\text{Accuracy} = 1 - |\,(C_{real} - C_{measured})/\,C_{real}\,| \tag{3}$$

where C_{real} is the actual concentration of the synthetic uric acid and $C_{measured}$ is the measured uric acid concentration obtained from the graph. All of these performances for each sample wavelength are plotted in Fig. 6 for ease of analysis. Fig. 6(a) shows the system linearity as a function of wavelength. In general, the system linearity is relatively low ($R^2 \approx 0.85$) for wide concentration uric acid at the light source operated less than 450nm wavelength. Then, it starts to improve significantly between 500nm to 850 nm with the R^2 value higher than 0.93, indicating a strong linear correlation. The highest linearity is observed at 950 nm wavelength with $R^2 = 0.9694$. In Fig. 6(b), the sensitivity performance shows that the system is highly sensitive at 435 nm wavelength with 0.006

$(mg/dL)^{-1}$. Then, the sensitivity performance dropped until 450 nm wavelength and started to increase and stabilize around 0.003 $(mg/dL)^{-1}$ between 500 to 800 nm wavelength. Above 850nm wavelength, the sensitivity starts to rise and reaches 0.004 $(mg/dL)^{-1}$ at 965nm wavelength. The highest sensitivity is at 435 nm with 0.00684 $(mg/dL)^{-1}$ sensitivity. As for the system accuracy, the calculated accuracy value for each sampled wavelength is plotted as in Fig. 6(c). Overall, the accuracy performance is higher than 95% for every sampled wavelength above 450nm with the highest accuracy achieved is 97.11% at 755nm wavelength. The system's linearity, sensitivity, and accuracy are outlined in Table 2 for ease of reference.

Table 2 *Summary of system performance (concentration from 10 to 200 mg/dL)*

Performance	Highest value	Lowest value
Linearity	0.9694 (950 nm)	0.7728 (435 nm)
Accuracy	98.01% (909 nm)	89.22% (435 nm)
Sensitivity $(mg/dL)^{-1}$	0.00684 (435 nm)	0.00203 (580 nm)

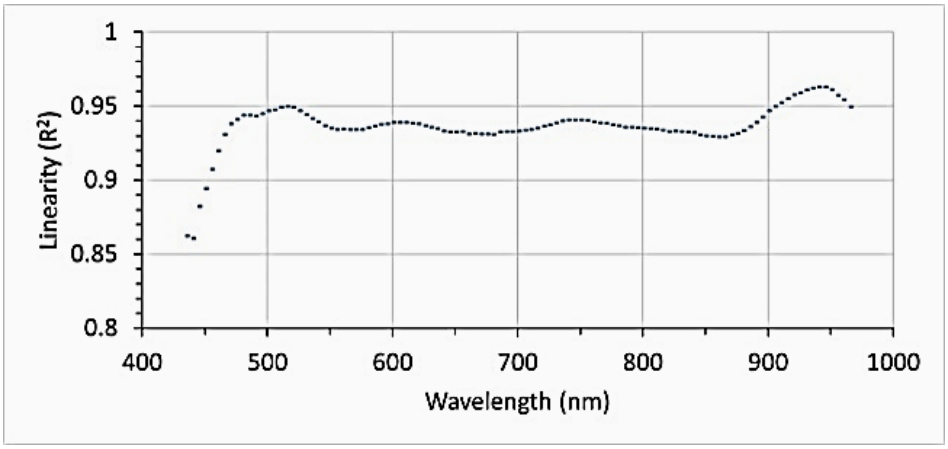

(a)

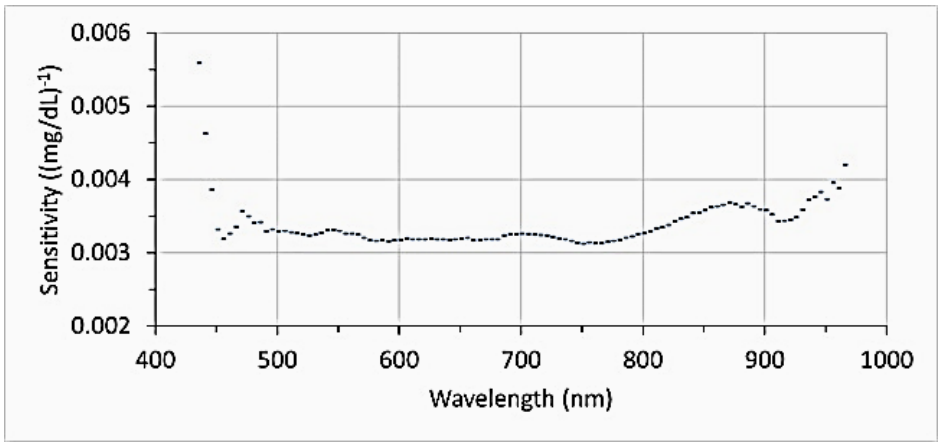

(b)

Int. Journal of Integrated Engineering Vol. 17 No. 6 (2025) p. 258-267

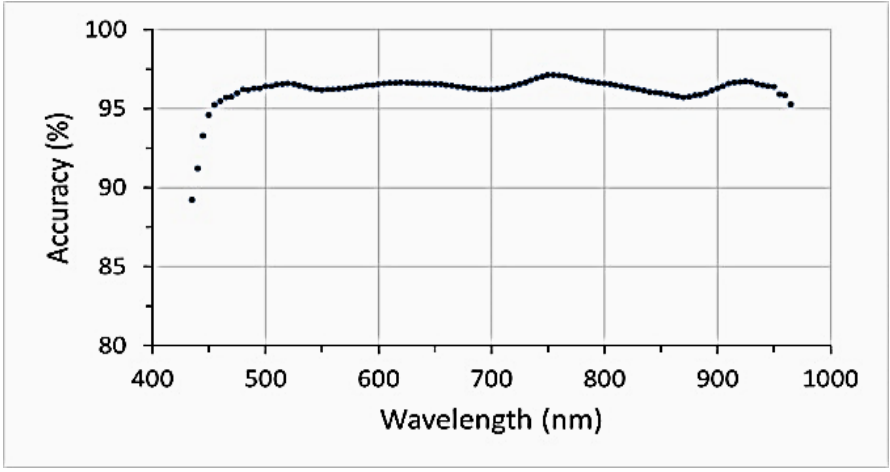

(c)

Fig. 6 *Performance analysis (light source wavelength range from 435 nm to 965 nm) in terms of (a) linearity; (b) sensitivity; and (c) accuracy*

Repeatability performance was investigated by analyzing its coefficient of variation or also known as relative standard deviation (RSD). It can be used to evaluate the performance of the sensor. The RSD is a value that is calculated by dividing the standard deviation, σ by the mean, μ value as given in equation (4) [35], [36].

$$\text{RSD} = \frac{\sigma}{\mu} \times 100 \tag{4}$$

To further evaluate the precision of the measurements, analysis was conducted at a wavelength of 950 nm across uric acid concentrations ranging from 10 to 200 mg/dL, as illustrated in Fig. 7. The relative standard deviation (RSD) for each concentration was computed using Equation 4 and subsequently plotted. The results indicate that the lowest RSD, 0.29%, occurred at 70 mg/dL, while the highest, 6.86%, was observed at 80 mg/dL. Overall, the average RSD across all tested concentrations remained below 3.11%, suggesting high consistency in the measurements. RSD, expressed as a percentage, provides insight into the precision of data by quantifying the degree of dispersion relative to the mean. Lower RSD values reflect greater consistency, whereas higher values denote increased variability in the dataset, aiding in the assessment of measurement reliability.

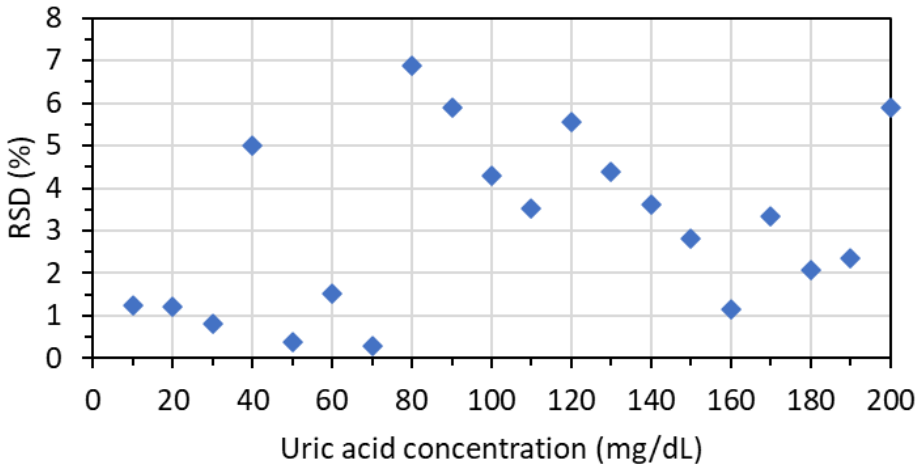

Fig. 7 *RSD performance (λ=950 nm)*

For further analysis, the findings of this study are compared with previous developments for both indirect and direct methods of uric acid detection in terms of linearity range, linearity, sensitivity and accuracy performances. These parameters are tabulated in Table 2. In general, indirect methods perform better than direct methods in the sense of sensitivity and linearity. However, in terms of linearity range and accuracy, the performances of the direct detection method are superior compared to the indirect methods. For comparison of

this work with the reported direct methods, the development in [37] that operates in the visible spectrum (650 nm wavelength) records a lower linearity range, linearity and accuracy. In this work, the linearity range is successfully enhanced, so the system can linearly detect the uric acid from 10 to 200 mg/dL. The enhancement is attributed to the use of optimal light source wavelength in the system. Specifically, the lower value of the molar attenuation coefficient in the wavelength offers a higher concentration range that can be detected by the spectrophotometer [30].

Table 2 *The comparison of the sensing performance of the proposed sensor with the previously developed sensor (high concentration UA)*

Mechanism	Linearity range	Sensitivity	Linearity	Accuracy
Indirect detection				
Colorimetric (CuNPs) (λ =520nm) [2]	0.08 – 76 mg/dL	0.0064 $(mg/dl)^{-1}$	0.9939	98.92 (%)
Colorimetric (unstable chromophore) (λ =520nm) [27]	2 – 10 mg/dL	0.0103 $(mg/dl)^{-1}$	0.9940	98.32 (%)
Spectroscopy (NaOH) (λ =460nm) [29]	15 - 85 mg/dL	0.0046 $(mg/dl)^{-1}$	0.9815	96.62 (%)
Spectroscopy (Ce^{4+} with methyl orange) (λ =505nm) [28]	0.007 – 0.231 mg/dL	4.2703 $(mg/dl)^{-1}$	0.8659	91.57 (%)
Direct detection				
Intensity modulated displacement sensor (λ =650 nm) [37]	0-50 mg/dL	0.0015 V/ppm	0.9394	94.32 (%)
Spectroscopy (λ =950 nm) [This work]	10-200 mg/dL	0.0034 $(mg/dl)^{-1}$	0.9694	97.42 (%)

4. Conclusion

This study successfully demonstrated a wide range of uric acid detection within the visible and NIR spectrum using a direct spectroscopy detection method. The system exhibits exceptional performance in terms of linearity, sensitivity, and accuracy within the 750nm to 950nm wavelength range. Analysis of the experimental results identified the optimal sensor performance at a wavelength of 950 nm, where the sensor achieved a wide linearity range from 10 to 200 mg/dL, with a linearity of 0.9694, a sensitivity of 0.0034 $(mg/dL)^{-1}$, and an accuracy of 97.42%. Compared to previous direct spectroscopy-based detection methods for a wide concentration range of uric acid, the proposed system demonstrates an extended linearity range up to 200 mg/dL and slight improvements in accuracy and sensitivity. Furthermore, the direct detection spectroscopy system operating in this spectrum offers the advantage of a faster response time, as it eliminates the need for enzymes or reagents in the detection process.

Acknowledgement

This research was fully supported by Ministry of Higher Education (MOHE) through the Fundamental Research Grant Scheme (FRGS) (FRGS/1/203/UTHM/02/5/2 K429)

Conflict of Interest

The manuscript has not been published elsewhere and is not under consideration by other journals. All authors have approved the review, agree with its submission and declare no conflict of interest on the manuscript

Author Contribution

The authors confirm contribution to the paper as follows: ***study conception and design:*** *Afiqah Yaacob, Nor Hafizah Ngajikin, Noran Azizan Cholan;* ***data collection:*** *Afiqah Yaacob;* ***analysis and interpretation of results:*** *Ian Yulianti, Nurfarina Zainal, Siti Hajar Aminah Ali, Maslina Yaacob;* ***draft manuscript preparation:*** *Afiqah Yaacob, Nor Hafizah Ngajikin. All authors reviewed the results and approved the final version of the manuscript.*

References

[1] Kumar, V., & Gill, K. D. (2018). To Determine the Uric Acid Concentration in Serum and Urine. In Basic Concepts in Clinical Biochemistry: A Practical Guide (pp. 81–84). Springer Singapore. https://doi.org/10.1007/978-981-10-8186-6_20

[2] Ma, C., Kong, L., Sun, X., Zhang, Y., Wang, X., Wei, X., Wan, H. & Wang, P. (2023). Enzyme-free and wide-range portable colorimetric sensing system for uric acid and hydrogen peroxide based on copper nanoparticles, *Talanta,* 255, 124196, https://doi.org/10.1016/j.talanta.2022.124196.

[3] Elagamy, S.H., Adly, L. & Abdel Hamid, M.A. (2023). Smartphone based colorimetric approach for quantitative determination of uric acid using Image J, *Scientific Reports*, 13 (21888), https://doi.org/10.1038/s41598-023-48962-0

[4] George, C., Leslie, S.W., & Minter, D.A. (2023, October 14). *Hyperuricemia*. StatPearls Publishing, Retrieved November 7, 2024, from https://www.ncbi.nlm.nih.gov/books/NBK459218/

[5] Prabhakar, A. P., & Lopez-Candales, A. (2024). Uric acid and cardiovascular diseases: a reappraisal. *Postgraduate Medicine*, 136(6), 615–623. https://doi.org/10.1080/00325481.2024.2377952

[6] Borghi, C., Rosei, E.A., Bardin, T., Dawson, J., Dominiczak, A., Kielstein, J.T., Manolis, A.J., Perez-Ruiz, F. & Mancia, G. (2015). Serum uric acid and the risk of cardiovascular and renal disease, *Journal of Hypertension*, 33(9), 1729–1741, https://doi.org/10.1097/HJH.0000000000000701

[7] Song, D., Zhao, X., Wang, F. & Wang, G. (2021). A brief review of urate transporter 1 (URAT1) inhibitors for the treatment of hyperuricemia and gout: Current therapeutic options and potential applications, *European Journal of Pharmacology*, 907, 174291, https://doi.org/10.1016/j.ejphar.2021.174291

[8] Barkas, F., Elisaf, M., Liberopoulos, E., Kalaitzidis, R. & Liamis, G. (2018). Uric acid and incident chronic kidney disease in dyslipidemic individuals. *Current Medical Research and Opinion,* 34(7), 1193–1199, https://doi.org/10.1080/03007995.2017.1372157

[9] Bhole, V., Choi, J.W.J., Kim, S.W., de Vera, M.& Choi, H. (2010) Serum uric acid levels and the risk of type 2 diabetes: a prospective study, *American Journal of Medicine,* 123(10), 957–961, https://doi.org/10.1016/j.amjmed.2010.03.027

[10] Johnson, R.J., Sanchez Lozada, L.G., Lanaspa, M.A., Piani, F. & Borghi, C. (2023) Uric Acid and Chronic Kidney Disease: Still More to Do, *Kidney International Report*, 8 (2), 229–239, https://doi.org/10.1016/j.ekir.2022.11.016

[11] Fu, L., Zhu, J. & Karimi-Maleh, H. (2021) An analytical method based on electrochemical sensor for the assessment of insect infestation in flour, *Biosensors (Basel)*, 11(9), 325, https://doi.org/10.3390/BIOS11090325

[12] Induja, C., Loganathan, M. & Naveen R. (2024). Development of paper-based strip to determine uric acid in wheat flour, *Journal of Cereal Research*, 16(2), 137-142. http://doi. org/10.25174/2582-2675/2024. 2024;150717

[13] Das, L., Das, S., Chandra, I.R., Kumar Mallick, A. & Gupta, A. (2021) Validation and comparison of analytical methods for the determination of uric acid in pulses and cereals by salting out assisted extraction by rapid resolution liquid chromatography, *Journal of Chromatography B*, 1180, 122894, https://doi.org/10.1016/j.jchromb.2021.122894

[14] Stathas, I.G., Sakellaridis, A.C., Papadelli, M., Kapolos, J., Papadimitriou, K. & Stathas, G.J. (2023) The Effects of Insect Infestation on Stored Agricultural Products and the Quality of Food, *Foods*, 12(10), 2046, https://doi.org/10.3390/foods12102046

[15] Gunasekaran, N., Baskaran, V. & Rajendran, S. (2003) Effect of Insect Infestation on Proximate Composition of Selected Stored Spice Products, *Journal of Food Science and Technology*, 40(2), 239–242

[16] Abrori, S.A., Septiani, N.L.W., Hakim, F.N., Maulana, A., Suyatman, Nugraha, Anshori, I. & Yuliarto, B. (2021) Non-Enzymatic Electrochemical Detection for Uric Acid Based on a Glassy Carbon Electrode Modified with MOF-71, *IEEE Sensor Journal*, 21(1), 170–177, https://doi.org/10.1109/JSEN.2020.3014298

[17] Yaitskikh, A.V., Zakladnoy, G.A. & Stepanenko, D.S. (2023) Increasing the efficiency of uric acid determination using HPLC. *Food processing industry,* 114–116

[18] Hamzah, H.H., Zain Z.M., Musa, N.L.W., Lin, Y.C. & Trimbee, E. (2013) Spectrophotometric Determination of Uric Acid in Urine Based-Enzymatic Method Uricase with 4-Aminodiphenylamine Diazonium Sulfate (Variamine Blue RT Salt), *Journal of Analytical and Bioanalytical Technique*, S7:011, https://doi.org/10.4172/2155-9872.S7-011

[19] Boroumand, S., Chamjangali, M.A. & Bagherian, G. (2017) Double injection/single detection asymmetric flow injection manifold for spectrophotometric determination of ascorbic acid and uric acid: Selection the optimal conditions by MCDM approach based on different criteria weighting methods, *Spectrochimica Acta Part A: Molecular and Biomolecular Spectroscopy,* 174, 203–213, https://doi.org/10.1016/j.saa.2016.11.031

[20] Ma, L., Niu, L., Wang, W., Kang, W. & Shi, H. (2014) Investigation of a novel Ag(III) chemiluminescence system and its mechanism for determination of uric acid in human urine, *Journal of Brazilian Chemical Society*, 25(5), https://doi.org/10.5935/0103-5053.20140050

[21] Lin, T.J., Yen, K.T., Chen, C.F., Yan, S.T., Su, K.W. & Chiang, Y.L. (2022) Label-Free Uric Acid Estimation of Spot Urine Using Portable Device Based on UV Spectrophotometry, *Sensors*, 22(8), 3009 https://doi.org/10.3390/s22083009

[22] Norazmi, N., Rasad, Z.R.A., Mohamad, M. & Manap, H. (2017) Uric acid detection using uv-vis spectrometer, *IOP Conference Series: Materials Science and Engineering, Institute of Physics Publishing*, 257, 012031, https://doi.org/10.1088/1757-899X/257/1/012031

[23] Deepak, D. (2025, January 21). How to select the right cuvette material for UV-Vis absorbance studies? lab-training. https://lab-training.com/select-right-cuvette-material-uv-vis-absorbance-studies/

[24] Anupongongarch, P., Kaewgun, T., O'reilly, J. & Khaomek, P. (2023) A Study On The Relation Between Digital Output And Uric Acid In Artificial Blood Solution By Using A Uric Acid Detector, *International Journal of Applied Biomedical Engineering*, 15(2), 38-44

[25] MSE Supplies (2024, October 16). Spectrophotometer Quartz Cuvettes (Cells) with 10mm Path Length. https://www.msesupplies.com/products/mse-pro-spectrophotometer-quartz-cuvettes-cells-with-10mm-path-length

[26] ITS Labshop (2024, October 16). UV-Cuvette. https://www.its-labshop.com.my/product/id/brand-uvc

[27] Induja, C., Loganathan, M. & Shanmugasundaram, S. (2022) Development Of A Simple Rapid Method For Determination Of Uric Acid Using UV Visible Spectroscopy, *International Journal of Life Science and Pharma Research,* 12(1), 200-205, https://doi.org/10.22376/ijpbs/lpr.2022.12.1.l200-205

[28] Hend Gamal Mousa & Khaleed Mansour Elgendy (2023) Spectrophotometric determination of uric acid in urine and blood samples, *Bulletin of Faculty of Science, Zagazig University,* 2023(1), 100–107, https://doi.org/10.21608/bfszu.2022.164109.1185

[29] Rashid, N.C.A., Ngajikin, N.H., Azmi, A.I., Arsat, R., Isaak, S., Cholan, N.A. & Azmi, N.E. (2019) Spectrophotometer with enhanced sensitivity for uric acid detection. *Chinese Optics Letters*, 17(8), 081701, https://doi.org/10.3788/col201917.081701

[30] Yaacob, A., Ngajikin, N.H., Rashid, N.C.A., Yaacob, M., Ali, S.H.A., Azmi, N.E. & Cholan, N.A. (2022) Linearity range enhancement in direct detection of low concentration uric acid. *Optik,* 249, 168243, https://doi.org/10.1016/j.ijleo.2021.168243

[31] Kim, J. (2015) Noninvasive Uric acid Monitoring Device using Near-Infrared Spectroscopy, *Journal of Biosensor and Bioelectronics, 6(4),* https://doi.org/10.4172/2155-6210.1000188

[32] Kahlet, N.A., Isa, N.M., Alauddin, S.M., Burham, N. & Saad, H. (2024) Enhancement of Sensing Performance for Alcohol in Aqueous Solution using Tapered Optical Fiber Coated with Polyaniline via Air-Brushing Technique, *International Journal of Integrated Engineering*, 16, 280–289, https://doi.org/10.30880/ijie.2024.16.07.025

[33] Yaacob, A., Ngajikin, N.H., Rashid, N.C.A., Ali, S.H.A., Yaacob, M., Isaak, S. & Cholan, N.A. (2020) Uric acid detection in visible spectrum, *Telecommunication Computing Electronics and Control (Telkomnika),* 18(4), 2035–2041, https://doi.org/10.12928/TELKOMNIKA.V18I4.14993.

[34] Rashid N.C.A., Cholan N.A., Tay K.G., Yaacob A., Sulaiman N.I., Mokhiri K. & Ngajikin N.H. (2022) Optimization of light source wavelength for ammonia detection in water, *Telecommunication Computing Electronics and Control (TELKOMNIKA)*, 20(5), 1132-1138, https://doi.org/10.12928/TELKOMNIKA.v20i5.24079.

[35] Everitt B.S. & Skrondal A. (2010). *The Cambridge Dictionary of Statistics*. 4th Edition. Cambridge University Press. https://www.stewartschultz.com/statistics/books/Cambridge%20Dictionary%20Statistics%204th.pdf

[36] Sukhpal Singh Gill, Peter Garraghan, Vlado Stankovski, Giuliano Casale, Ruppa K. Thulasiram, Soumya K. Ghosh, Kotagiri Ramamohanarao & Rajkumar Buyya (2019) Holistic resource management for sustainable and reliable cloud computing: An innovative solution to global challenge, *Journal of Systems and Software*, 155, 104-129, https://doi.org/10.1016/j.jss.2019.05.025

[37] Gan, N.N.G.M.A., Taib, N.A.M., Abdullah, M., Mukhtar, W.M. & Rashid, A.R.A. (2019) Uric acid detection by using contactless intensity modulation based displacement sensor, *Journal of Physics: Conference Series*, 1371, 1-6, https://doi.org/10.1088/1742-6596/1371/1/012020